

Title	Stokesian flow of a micropolar fluid past a sphere
Sub Title	
Author	澤田, 達男(Sawada, Tatsuo) 鎌田, 敏弘(Kamata, Toshihiro) 棚橋, 隆彦(Tanahashi, Takahiko) 安藤, 常世(Ando, Tsuneyo)
Publisher	慶應義塾大学工学部
Publication year	1983
Jtitle	Keio Science and Technology Reports Vol.36, No.4 (1983. 8) ,p.33- 47
JaLC DOI	
Abstract	A creeping flow of micropolar fluids past a sphere is presented by using a vector potential. As a boundary condition, an intermediate spin condition between zero spin and one-half of vorticity is used. Analytical expressions for velocity, vorticity, microrotation in the flow field and drag on the sphere are obtained, which are completely characterized by three dimensionless parameters, i.e. the ratio of vortex viscosity to shear viscosity, the size effect parameter of corpuscles to the sphere and the wall-condition parameter. Characteristics of steady flows past a sphere is investigated for these parameters. The viscosity ratio represents a polar effect which occurs between corpuscles and fluid. The size effect parameter means the ratio of a corpuscle to the radius of a sphere. When the wall-condition parameter varies from no-spin condition to equi-vorticity condition, the microrotation changes in the whole region. The ratio of pressure drag to frictional drag in a micropolar fluid is one to two. This value is the same one for Newtonian fluid.
Notes	
Genre	Departmental Bulletin Paper
URL	<a href="https://koara.lib.keio.ac.jp/xoonips/modules/xoonips/detail.php?koara_id=KO50001004-00360004-0033">https://koara.lib.keio.ac.jp/xoonips/modules/xoonips/detail.php?koara_id=KO50001004-00360004-0033</a>

慶應義塾大学学術情報リポジトリ(KOARA)に掲載されているコンテンツの著作権は、それぞれの著作者、学会または出版社/発行者に帰属し、その権利は著作権法によって保護されています。引用にあたっては、著作権法を遵守してご利用ください。

The copyrights of content available on the KeiO Associated Repository of Academic resources (KOARA) belong to the respective authors, academic societies, or publishers/issuers, and these rights are protected by the Japanese Copyright Act. When quoting the content, please follow the Japanese copyright act.

## STOKESIAN FLOW OF A MICROPOLAR FLUID PAST A SPHERE

Tatsuo SAWADA\*, Toshihiro KAMATA\*\*, Takahiko TANAHASHI\*\*\*  
and Tsuneyo ANDO\*\*\*\*

Department of Mechanical Engineering, Keio University,  
Hiyoshi, Yokohama 223, Japan

*(Received, April 2, 1983)*

### ABSTRACT

A creeping flow of micropolar fluids past a sphere is presented by using a vector potential. As a boundary condition, an intermediate spin condition between zero spin and one-half of vorticity is used. Analytical expressions for velocity, vorticity, microrotation in the flow field and drag on the sphere are obtained, which are completely characterized by three dimensionless parameters, i.e. the ratio of vortex viscosity to shear viscosity, the size effect parameter of corpuscles to the sphere and the wall-condition parameter. Characteristics of steady flows past a sphere is investigated for these parameters. The viscosity ratio represents a polar effect which occurs between corpuscles and fluid. The size effect parameter means the ratio of a corpuscle to the radius of a sphere. When the wall-condition parameter varies from no-spin condition to equi-vorticity condition, the microrotation changes in the whole region. The ratio of pressure drag to frictional drag in a micropolar fluid is one to two. This value is the same one for Newtonian fluid.

### 1. Introduction

Recently, theoretical treatment of the mechanical behaviors of a fluid which possesses substructures, such as dilute polymer liquids, bloods, fluid suspensions etc., has developed in considerable attentions. Classical continuum mechanics is based on the idea that all material bodies possess continuous mass densities, and that constitutive equations are valid for every part of a body regardless of its size. However, this postulate is doubtful in the treatment of a fluid which possess substructures. As the size of a material volume element is allowed to approach zero, one finds that, past a certain critical volume, the mass density begins to show a dependence on its volume and the continuity assumption for mass density is no longer applicable. Since the macroscopic limitation of the material volume element

---

\* Research Assistant

\*\* Research Engineer, Mitsubishi Heavy Industry Co., Ltd.

\*\*\* Associate Professor

\*\*\*\* Professor

exists, the stress tensor is no longer symmetric. Hence there arise distributed couples per unit area across internal surfaces, i.e. couple stresses.

Considering a fluid which possesses substructures, it is necessary to take account of the intrinsic motion of the material constituents. Considering spin angular momentum, symmetry of the stress tensor is not assured, i.e. Cauchy's second law of motion is no longer valid.

A strong motivation for extending the range of applicability of continuum mechanics, particularly in the study of fluid dynamics, was the desire of engineers to treat such rheologically complex fluids. Several aspects as to classical continuum mechanics are reappraised and consequently the inadequacy of the classical continuum approach to describe the mechanics of complex fluids has led to develop the theories of microcontinua in which continuous media possess not only mass and velocity but also a substructure with which is associated a moment-of-inertia density and a microdeformation. These complex fluids are generically called microcontinuum fluids.

Many studies of microcontinuum fluids have been performed in various fields. Kline, Allen and DeSilva (1968)<sup>(15)</sup>, Cowin (1972)<sup>(10)</sup> and Ariman (1971)<sup>(4)</sup> applied a continuum approach to Poiseuille flow of blood. Kline and Allen (1969)<sup>(14)</sup>, and Kline, Allen and Keshavarzi (1972)<sup>(16)</sup> investigated the concentration effects of red cells in oscillatory blood flows. Ariman, Turk and Sylvester (1974)<sup>(5)</sup> compared the theoretical velocity profiles with the experimentally determined profiles for both steady and pulsatile blood flows. Allen, Kline and Ling (1971)<sup>(3)</sup> investigated the ability of microcontinuum fluid theories to explain the behavior of polyisobutylene. Ferromagnetic fluid is a stable suspension of fine particles of a solid ferromagnetic material such as magnetite in nonconducting liquids, e.g. water and kerosene. Neuringer and Rosensweig (1964)<sup>(18)</sup> and Shliomis (1972)<sup>(20)</sup> studied ferromagnetic fluid basically. Brenner (1970)<sup>(6)</sup>, and Brenner and Weissman (1972)<sup>(7)</sup> presented theoretical analysis of the effects of an external magnetic field on the rheological properties of a ferrofluid. McTague (1969)<sup>(17)</sup>, Kamiyama, Koike and Iizuka (1979)<sup>(12)</sup>, and Tomita et al. (1981)<sup>(24)</sup> have investigated the flow behavior experimentally. Tanahashi et al. (1983)<sup>(23)</sup> have considered the steady flow of a ferromagnetic fluid in the basis of the micropolar theory which was suggested by Eringen (1966)<sup>(11)</sup>.

Though the approach of microcontinuum fluids is very useful to treat complex fluids, various problems have been unsolved. For example, the spin boundary condition is not clarified. The classical no-slip boundary condition was assumed for velocity, whereas a variety of boundary conditions have been applied to the microrotation. Experimental considerations are necessary to conclude what kind of boundary condition is fit for. There is also a problem of determination of material constants, when the microcontinuum theory is applied to real flow problems. An attempt for the determination of material constants has not been made fully, yet.

In the present paper, the authors use the theory of micropolar fluid, which is thought to be most fundamental in microcontinuum fluids. The Stokesian flow of a micropolar fluid past a fixed sphere is examined. By introducing the stream function and the axisymmetrical potential operator, Ramkissoon and Majumdar (1975)<sup>(19)</sup> have solved this problem. It has been also investigated by Aero, Bulygin

and Kuvshinskii (1965)<sup>(1)</sup> using asymmetric hydrodynamics which is a generalization of the ordinary hydrodynamics for the case in which the stress tensor becomes asymmetric, and by Stokes (1971)<sup>(27)</sup> using the theory developed for couple stress fluids. But detailed discussions about flow behaviors were not carried out in these investigations. Here, by introducing the vector potential and drawing stream lines, equi-microrotation lines and equi-vorticity lines, the authors clarify the flow behaviors near the sphere. An intermediate boundary condition is introduced and characteristics of dimensionless parameters are discussed in detail.

## 2. Formulation of the Problem

### 2.1 Fundamental equations

The equations which express the conservation of mass, momentum and angular momentum for micropolar fluids are

$$\frac{d\rho}{dt} + \rho \operatorname{div} \mathbf{v} = 0, \quad (1)$$

$$\rho \frac{d\mathbf{v}}{dt} = -\nabla p + (\lambda + 2\mu)\nabla\nabla \cdot \mathbf{v} - (\mu + \mu_1)\nabla \times \nabla \times \mathbf{v} + 2\mu_1\nabla \times \boldsymbol{\Omega} + \rho \mathbf{b}, \quad (2)$$

$$\frac{\rho\gamma}{\mu} \frac{d\boldsymbol{\Omega}}{dt} = (\alpha + \beta + \gamma)\nabla\nabla \cdot \boldsymbol{\Omega} - \gamma\nabla \times \nabla \times \boldsymbol{\Omega} + 2\mu_1\nabla \times \mathbf{v} - 4\mu_1\boldsymbol{\Omega} + \rho \mathbf{l}, \quad (3)$$

where  $\mathbf{v}$ ,  $\boldsymbol{\Omega}$ ,  $\mathbf{b}$ ,  $\mathbf{l}$ , and  $t$  are velocity vector, microrotation vector, body force vector, body couple vector, and time, respectively;  $\rho$  is the mass density,  $\lambda$  is the second viscosity,  $\mu$  is the shear viscosity, and  $\mu_1$  is the vortex viscosity which is a proportionality constant in the antisymmetric part of stress tensor. Furthermore,  $\alpha$ ,  $\beta$  and  $\gamma$  are material constants which are called spin viscosities.

### 2.2 Flow past a sphere

Consider the slow steady flow streaming in the negative  $z$  direction with uniform velocity  $U$  in the infinite distance from a sphere of radius  $a$ . Taking spherical coordinates as shown in Fig. 1, the fluid motion is assumed to be axisym-

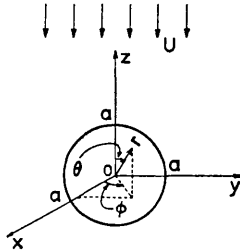


Fig. 1. Flow past a sphere

metric and independent of the azimuthal angle  $\phi$ . Hence, velocity, vorticity and microrotation vectors are respectively written as

$$\mathbf{v}=(v_r, v_\theta, 0), \quad \boldsymbol{\omega}=(0, 0, \omega_\phi), \quad \boldsymbol{\Omega}=(0, 0, \Omega_\phi). \quad (4)$$

Using Eq. (4), the following equations are established.

$$\nabla \cdot \boldsymbol{\omega}=0, \quad \nabla \cdot \boldsymbol{\Omega}=0. \quad (5)$$

From now on, the authors write  $\omega_\phi$  and  $\Omega_\phi$  in brief as  $\omega$  and  $\Omega$ . Non-dimensional starred quantities are introduced by the following relations

$$\left. \begin{aligned} A^* &= A/aU, & \Psi^* &= \Psi/a^2U, & D^* &= D/6\pi\mu Ua, \\ \omega^* &= \omega/(U/a), & \Omega^* &= \Omega/(U/a), & p^* &= p/(\mu U/a), \\ r^* &= r/a, & v_r^* &= v_r/U, & v_\theta^* &= v_\theta/U. \end{aligned} \right\} \quad (6)$$

Here,  $A$ ,  $\Psi$  and  $D$  are the azimuthal component of vector potential, the stream function and the drag acting on a sphere in the direction of the negative  $z$  axis, respectively. Their analytical expressions will be described later on. For simplicity, let us drop the asterisks indicating the non-dimensional quantities. Substituting Eqs. (4) and (6) into Eqs. (1), (2) and (3) leads to

$$\nabla \cdot \mathbf{v}=0, \quad (7)$$

$$-\nabla p - (1 + \varepsilon)\nabla \times \boldsymbol{\omega} + 2\varepsilon\nabla \times \boldsymbol{\Omega} = 0, \quad (8)$$

$$\frac{2}{\lambda^2(1 + \varepsilon)}\nabla^2 \boldsymbol{\Omega} + \boldsymbol{\omega} - 2\boldsymbol{\Omega} = 0, \quad (9)$$

where

$$\varepsilon = \mu_1/\mu, \quad \lambda = \sqrt{4\mu\mu_1/\gamma(\mu + \mu_1)} \cdot a. \quad (10)$$

$\varepsilon$  is the ratio of viscosities and  $\lambda$  the size effect parameter.

### 2.3 Vector potential

Axisymmetrical flow problems are usually solved by Stokes' stream function, but the authors use a vector potential instead of it because the latter is considered to be more essential than the former. From Eq. (7), the vector potential  $\mathbf{A}$  is introduced by

$$\mathbf{v} = \nabla \times \mathbf{A}. \quad (11)$$

From Eq. (4),  $\mathbf{A}$  has only the azimuthal component, therefore,

$$\mathbf{A} = A(r, \theta)\mathbf{e}_\phi. \quad (12)$$

Then Eq. (12) leads to the zero divergence of  $\mathbf{A}$ :

$$\nabla \cdot \mathbf{A} = 0. \quad (13)$$

By using Eqs. (11) and (12), Eqs. (8) and (9) yield the following equation :

$$G^4(G^2 - \lambda^2)A = 0, \quad (14)$$

here,  $G^2$  is the operator given by

$$G^2 = \nabla^2 - \frac{1}{r^2 \sin^2 \theta}. \quad (15)$$

Each component of velocity, vorticity and microrotation can be expressed by the vector potential and the  $G^2$ -operator. That is,

$$v_r = \frac{1}{r \sin \theta} \cdot \frac{\partial}{\partial \theta} (\sin \theta \cdot A), \quad (16)$$

$$v_\theta = -\frac{1}{r} \cdot \frac{\partial}{\partial r} (rA), \quad (17)$$

$$\omega = -G^2 A, \quad (18)$$

$$\Omega = -\frac{1}{2} \left( G^2 A + \frac{1}{\epsilon \lambda^2} G^4 A \right). \quad (19)$$

### 3. Boundary Conditions

For velocity, the no-slip condition on the surface of the sphere and the uniform flow condition at infinity require that

$$r=1; \quad v_r = v_\theta = 0, \quad (20)$$

$$r \rightarrow \infty; \quad v_r \rightarrow -\cos \theta, \quad v_\theta \rightarrow \sin \theta. \quad (21)$$

Using the vector potential, Eqs. (20) and (21) are expressed by

$$r=1; \quad \frac{\partial}{\partial \theta} (\sin \theta \cdot A) = 0, \quad \frac{\partial}{\partial r} (rA) = 0, \quad (22)$$

$$r \rightarrow \infty; \quad A = -\frac{1}{2} r \sin \theta. \quad (23)$$

On the other hand, various arguments have been made for spin boundary condition, but a clear conclusion has not been obtained yet. A variety of boundary conditions have been applied to the microrotation. The most common boundary condition assumed for the microrotation is the no-spin condition at the wall which requires the microelements of fluid to adhere to a solid boundary without rotation. This boundary condition is used by Eringen (1966). However, experimental results, for example, of Bugliarello and Sevilla (1970)<sup>(8)</sup> on blood flow in rigid tubes indicated that red blood cells rotate on the wall of tubes.

More general boundary condition for the microrotation has been studied by Kirwan and Newman (1969)<sup>(13)</sup>. They assumed microrotation to be an indefinable

at the wall. This is nothing but mathematically appealing from the point of view that analytical solutions are possible, and there is no way to determine such a constant.

Ariman, Turk and Sylvester (1974) presented another boundary condition which is in the form of the vanishing of a microrotation gradient at the wall. This is based on the experimental consideration of Bugliarello and Sevilla (1970). Since the microrotation gradient equals zero at the wall, the microrotation has an arbitrary constant at the wall. Hence, this boundary condition is called the constant-spin condition and is analogous to that proposed by Kirwan and Newman in a sense.

Allen and Kline (1968)<sup>(2)</sup> investigated the influence of two spin boundary conditions on a simple shear flow. One of them is that microrotation and fluid vorticity are identical at the wall. In this case, solutions are indistinguishable from those of Newtonian fluid. The other is the opposite extreme, i.e. the no-spin boundary condition. Thus Allen and Kline considered an intermediate spin boundary condition between the above two extremes, which was first suggested by Condiff and Dahler (1964)<sup>(9)</sup>, namely,

$$\Omega = \frac{1}{2} \delta \omega, \quad (24)$$

where  $\delta$  is the wall-condition parameter, which depends on the surface condition of the wall, flow behavior and the concentration of corpuscles.

As mentioned above, some spin boundary conditions have been proposed by many researchers. Here, the authors use the intermediate boundary condition for microrotation, that is,

$$r=1; \quad \Omega = \frac{1}{2} \delta \omega \quad (0 < \delta < 1). \quad (25)$$

Here  $\delta$  ranges over the interval  $0 < \delta < 1$ , and when  $\delta=0$ ,  $\Omega=0$  on the sphere, i.e. the no-spin boundary condition in result. When  $\delta=1$ , the antisymmetric stress vanishes on the sphere. In terms of the vector potential, Eq. (25) is rewritten by

$$r=1; \quad (1-\delta)G^2 A + \frac{1}{\varepsilon \lambda^2} G^4 A = 0. \quad (26)$$

#### 4. Mathematical Solutions

After substitution of Eqs. (22), (23) and (26) into Eq. (14), and some straightforward manipulation, the solutions for  $A, v_r, v_\theta, \omega$  and  $\Omega$  are found as follows:

$$A = -\frac{r \sin \theta}{2} \left\{ \frac{1}{2r^3} - \frac{3}{2r} + 1 + \frac{B_1}{2r^3} - \frac{3B_2}{2r} - \frac{B_3}{r^2} \left( \lambda + \frac{1}{r} \right) e^{-\lambda r} \right\}, \quad (27)$$

$$v_r = -\frac{\cos \theta}{2} \left\{ \frac{1}{r^3} - \frac{3}{r} + 2 + \frac{B_1}{r^3} - \frac{3B_2}{r} - \frac{2B_3}{r^2} \left( r + \frac{1}{r} \right) e^{-\lambda r} \right\}, \quad (28)$$

$$v_\theta = -\frac{\sin \theta}{4} \left[ \frac{1}{r^3} + \frac{3}{r} - 4 - \frac{B_1}{r^3} + \frac{3B_2}{r} - \frac{2B_3}{r} \left\{ \frac{1}{r^2} + \lambda \left( \lambda + \frac{1}{r} \right) \right\} e^{-\lambda r} \right], \quad (29)$$

$$\omega = \frac{\sin \theta}{2} \left\{ \frac{3}{r^2} + \frac{3B_2}{r^2} - \frac{\lambda^2 B_3}{r} \left( \lambda + \frac{1}{r} \right) e^{-\lambda r} \right\}, \quad (30)$$

$$\Omega = \frac{\sin \theta}{4} \left\{ \frac{3}{r^2} + \frac{3B_2}{r^2} - \frac{\lambda^2(1+\varepsilon)B_3}{\varepsilon r} \left( \lambda + \frac{1}{r} \right) e^{-\lambda r} \right\}, \quad (31)$$

where

$$B_1 = \frac{3(\lambda^2 + 2\lambda + 2)\varepsilon(1-\delta)}{\lambda^2[\lambda\{\varepsilon(1-\delta)+1\}+1]}, \quad (32)$$

$$B_2 = \frac{\varepsilon(1-\delta)}{\lambda\{\varepsilon(1-\delta)+1\}+1}, \quad (33)$$

$$B_3 = \frac{3\varepsilon(1-\delta)e^\lambda}{\lambda^2[\lambda\{\varepsilon(1-\delta)+1\}+1]}. \quad (34)$$

The pressure can be obtained by utilizing Eqs. (30) and (31). The integration of Eq. (8) results in

$$p - p_\infty = \frac{3(1+B_2)}{2} \cdot \frac{\cos \theta}{r^2}, \quad (35)$$

where  $p_\infty$  is the uniform pressure at infinity.

Each component of stress and couple stress can be calculated by these solutions. The non-dimensional expressions of stress tensor and couple stress tensor are defined by

$$\begin{aligned} T_{ij}^* &= T_{ij}/(\mu U/a), \\ M_{ij}^* &= M_{ij}/(\gamma U/a^2), \end{aligned}$$

and again the authors omit the asterisks. Then each component of stress and couple stress can be expressed in the form

$$T_{rr} = -p_\infty + \cos \theta \left\{ \frac{3(1+B_1)}{r^4} - \frac{9(1+B_2)}{2r^2} - 2B_3 \left( \frac{3}{r^4} + \frac{3\lambda}{r^3} + \frac{\lambda^2}{r^2} \right) e^{-\lambda r} \right\}, \quad (36)$$

$$T_{r\theta} = \sin \theta \left\{ \frac{3(1+B_1)}{2r^4} - B_3 \left( \frac{3}{r^4} + \frac{3\lambda}{r^3} + \frac{\lambda^2}{r^2} \right) e^{-\lambda r} \right\}, \quad (37)$$

$$T_{\theta r} = \sin \theta \left\{ \frac{3(1+B_1)}{2r^4} - B_3 \left( \frac{3}{r^4} + \frac{3\lambda}{r^3} + \frac{2\lambda^2}{r^2} + \frac{\lambda^3}{r} \right) e^{-\lambda r} \right\}, \quad (38)$$

$$T_{\theta\theta} = -p_\infty - \cos \theta \left\{ \frac{3(1+B_1)}{2r^4} - B_3 \left( \frac{3}{r^4} + \frac{3\lambda}{r^3} + \frac{\lambda^2}{r^2} \right) e^{-\lambda r} \right\}, \quad (39)$$



$$T_{\phi\phi} = -p_\infty - \cos\theta \left\{ \frac{3(1+B_1)}{2r^4} - B_3 \left( \frac{3}{r^4} + \frac{3\lambda}{r^3} + \frac{\lambda^2}{r^2} \right) e^{-\lambda r} \right\}, \quad (40)$$

$$T_{r\phi} = T_{\theta\phi} = T_{\phi r} = T_{\phi\theta} = 0, \quad (41)$$

$$M_{r\phi} = -\frac{\sin\theta}{4} \left[ \frac{3(1+B_2)(2+\kappa)}{r^3} - \frac{\lambda^2(1+\varepsilon)B_3}{\varepsilon} \left\{ \frac{2+\kappa}{r^3} + \frac{\lambda(2+\kappa)}{r^2} + \frac{\lambda^2}{r} \right\} e^{-\lambda r} \right], \quad (42)$$

$$M_{\theta\phi} = \frac{(\cos\theta - \kappa \sin\theta \cot\phi)}{4} \left\{ \frac{3(1+B_2)}{r^3} - \frac{\lambda^2(1+\varepsilon)B_3}{\varepsilon} \left( \frac{\lambda}{r^2} + \frac{1}{r^3} \right) e^{-\lambda r} \right\}, \quad (43)$$

$$M_{\phi r} = -\frac{\sin\theta}{4} \left\{ \frac{3(2\kappa+1)(1+B_2)}{r^3} - \frac{\lambda^2(1+\varepsilon)B_3}{\varepsilon} \left( \frac{2\kappa+1}{r^3} + \frac{(2\kappa+1)\lambda}{r^2} + \frac{\kappa\lambda^2}{r} \right) e^{-\lambda r} \right\}, \quad (44)$$

$$M_{\phi\theta} = \frac{(\kappa \cos\theta - \sin\theta \cot\phi)}{4} \left\{ \frac{3(1+B_2)}{r^3} - \frac{\lambda^2(1+B_3)}{\varepsilon} \left( \frac{\lambda}{r^2} + \frac{1}{r^3} \right) e^{-\lambda r} \right\}, \quad (45)$$

$$M_{rr} = M_{r\theta} = M_{\theta r} = M_{\theta\theta} = M_{\phi\phi} = 0, \quad (46)$$

where  $\kappa$  is  $\kappa = \beta/\gamma$ . Naturally, the stress tensor expressed by Eqs. (37) and (38) is asymmetric.

## 5. Discussions

Solutions obtained in the preceding section are wholly characterized by three parameters, i.e.  $\varepsilon$  and  $\lambda$  defined in Eq. (10), and  $\delta$  defined in Eq. (25).

### 5.1 Velocity profiles

Each component of velocity in  $r$  and  $\theta$  directions is shown in Figs. 2, 3 and 4. These figures show the considerable influence of each parameter on velocity profiles. In the theory of micropolar fluid, it must be considered that corpuscles rotate because of shearing stresses. These rotations produce the microrotation, which has a relation with a volume averaged radius of gyration of a microelement. If the radius of a sphere changes, the velocity profile varies. In Newtonian fluid the

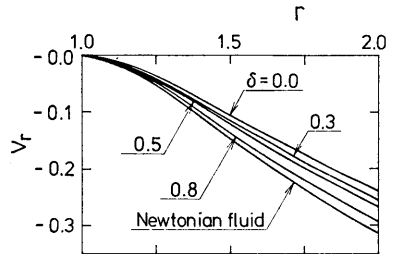
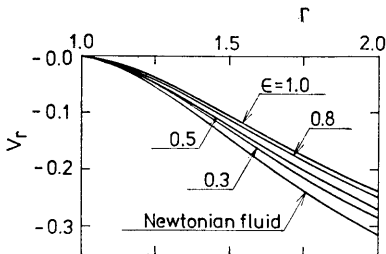
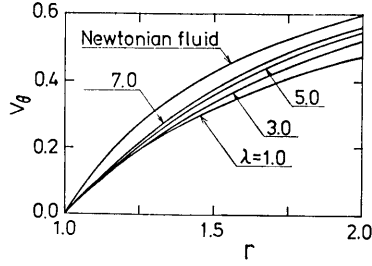


Fig. 2. Velocity profiles ( $\theta=0^\circ$ ,  $\lambda=1.0$ ,  $\delta=0.0$ ) Fig. 3. Velocity profiles ( $\theta=0^\circ$ ,  $\lambda=1.0$ ,  $\varepsilon=1.0$ )


 Fig. 4. Velocity profiles ( $\theta=90^\circ$ ,  $\varepsilon=1.0$ ,  $\delta=0.0$ )

velocity profile does not depend on the non-dimensional radius of a sphere. Such size effect corresponds to  $\lambda$ . Now let  $\lambda \rightarrow \infty$ , i.e. the ratio of a sphere to corpuscle radii be very large, then the velocity profile approaches that of Newtonian fluid. As  $\varepsilon$  becomes small, the velocity profile goes to that of Newtonian fluid. Vortex viscosity is a proportionality constant in the antisymmetric part of stress tensor which is yielded by the difference between one-half of vorticity and microrotation.  $\varepsilon$  going to zero corresponds to the decrease of vortex viscosity. Then, the antisymmetric part of stress tensor will be vanished in the limit. The micropolar effect does not appear in such a case. When  $\delta$  goes to 1, the velocity profiles also become those of Newtonian fluid. In the case of  $\delta=1$ , Eq. (25) reveals that the microrotation is identical to one-half of vorticity on the sphere. From Eqs. (30) and (31),  $\Omega$  and  $\omega/2$  are also equal everywhere, so that the asymmetry of stress tensor vanishes and the velocity profiles of micropolar fluid are identical to those of Newtonian fluid.

In Fig. 1, the authors adopt the convention that the algebraic sign of a volumetric flow rate is positive when the flow is in the direction of the negative  $z$  axis. Then, the relation between stream function  $\Psi$  and vector potential  $\mathbf{A}$  is given by

$$\mathbf{A} = -\frac{\mathbf{e}_\phi}{r \sin \theta} \Psi, \quad (47)$$

so that

$$\Psi = -r \sin \theta \cdot A. \quad (48)$$

Substituting Eq. (27) into Eq. (48) leads to

$$\Psi = \frac{r^2 \sin^2 \theta}{2} \left\{ \frac{1}{2r^3} - \frac{3}{2r} + 1 + \frac{B_1}{2r^3} - \frac{3B_2}{2r} - \frac{B_3}{r^2} \left( \lambda + \frac{1}{r} \right) e^{-\lambda r} \right\}. \quad (49)$$

Typical stream lines for both micropolar and Newtonian fluids are depicted in Fig. 5, in which the subscript  $n$  indicates Newtonian fluid. There is hardly significant difference of stream lines between micropolar and Newtonian fluids.

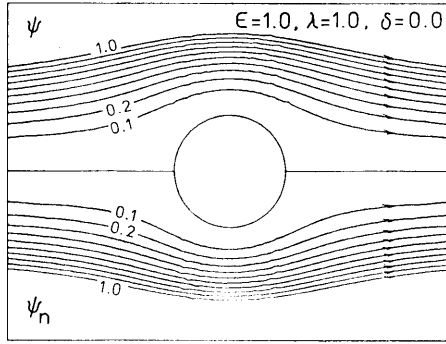


Fig. 5. Stream lines

5.2 Distributions of microrotation and vorticity

Equi-microrotation lines for two values of  $\epsilon$  (i.e.  $\epsilon=1.0$  and  $0.05$ ) are shown in Fig. 6. It is seen that distributions of microrotation are scarcely altered with  $\epsilon$ . In order to examine the influence of  $\epsilon$  on microrotation, distributions of microrotation in the radial direction ( $\theta=90^\circ$ ) are shown in Fig. 7. From this figure, the effect of  $\epsilon$  on microrotation is very significant on the surface of the sphere. Let denote the microrotation on the wall by  $\Omega_w$ . Then  $\Omega_w$  is given by

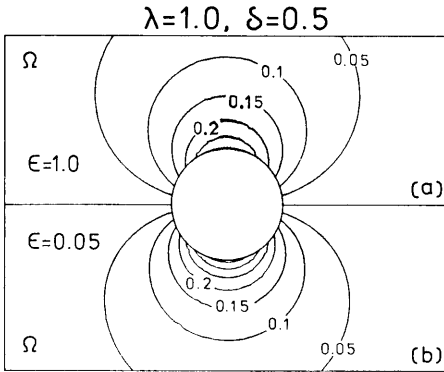


Fig. 6. Equi-microrotation lines

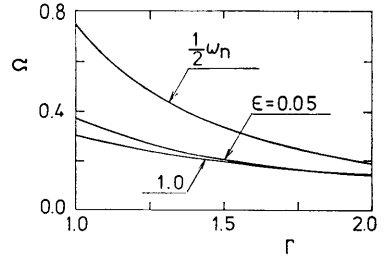


Fig. 7. Distributions of microrotation ( $\theta=90^\circ, \lambda=1.0, \delta=0.5$ )

$$\Omega_w = \frac{3 \sin \theta}{4} \cdot \frac{\delta(1+\lambda)}{\lambda\{\epsilon(1-\delta)+1\}} \tag{50}$$

Since  $\epsilon < 1$  and  $\delta < 1$ , then there only occurs a little change of  $\Omega_w$  in the wide range of  $\epsilon$ . Hence,  $\epsilon$  does not mean the friction between the wall and the fluid, but the friction between the corpuscle and the fluid.

Figures 8 (a, b, c) show the equi-microrotation lines with  $\lambda$  and Fig. 8 (d) shows

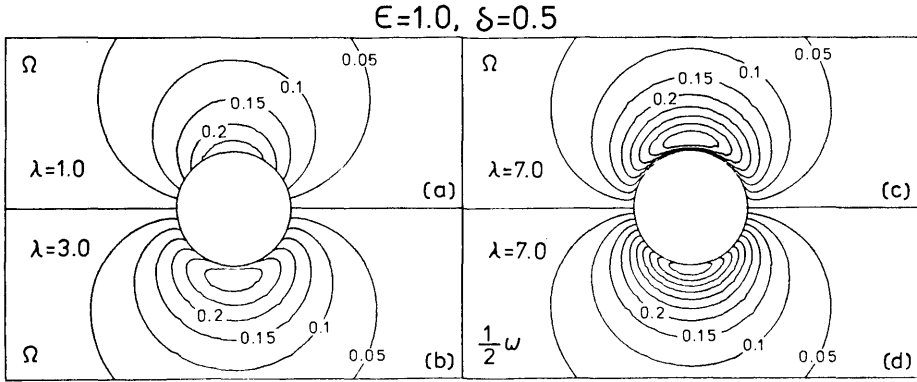


Fig. 8. Equi-microrotation lines

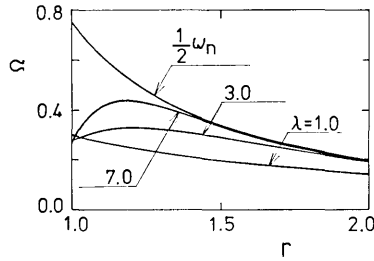


Fig. 9. Distributions of microrotation ( $\theta=90^\circ, \epsilon=1.0, \delta=0.5$ )

the one-half equi-vorticity lines. Distributions of microrotation in the radial direction ( $\theta=90^\circ$ ) are shown in Fig. 9 for  $\lambda$ . As  $\lambda$  becomes large,  $\Omega \rightarrow \omega/2$ , further  $\Omega \rightarrow \omega_n/2$ . In Figs. 8 (b, c), “crescents” appear in the neighborhood of the sphere. They correspond to the local maximum points in Fig. 9. When  $\lambda$  becomes large, the local maximum point approaches to the sphere and the domain of  $\Omega \approx \omega/2$  expands toward the sphere. In other words, the area over which the microrotation on the sphere spreads decreases, and  $\Omega \approx \omega_n/2$  appears almost in the whole area. But when  $\lambda \rightarrow \infty$  in Eq. (50), it follows that

$$\Omega_w \rightarrow \frac{3 \sin \theta}{4} \cdot \frac{1}{r^3} \cdot \frac{\delta}{1 + \epsilon(1 - \delta)}. \quad (51)$$

The influence of  $\epsilon$  and  $\delta$  remains only on the sphere. Then it seems that  $\lambda$  represents the behavior of the diffusion of microrotations on the sphere.

Equi-microrotation lines for four values of  $\delta$  are depicted in Fig. 10. Figure 11 shows the distributions of microrotation in the radial direction ( $\theta=90^\circ$ ). Though  $\delta$  is introduced in order to take account of the wall effect, the whole spin field alters sensitively with  $\delta$ . From Fig. 11, it is seen that  $\Omega \rightarrow \omega_n/2$  as  $\delta \rightarrow 1$ . So that the following equation is obtained;

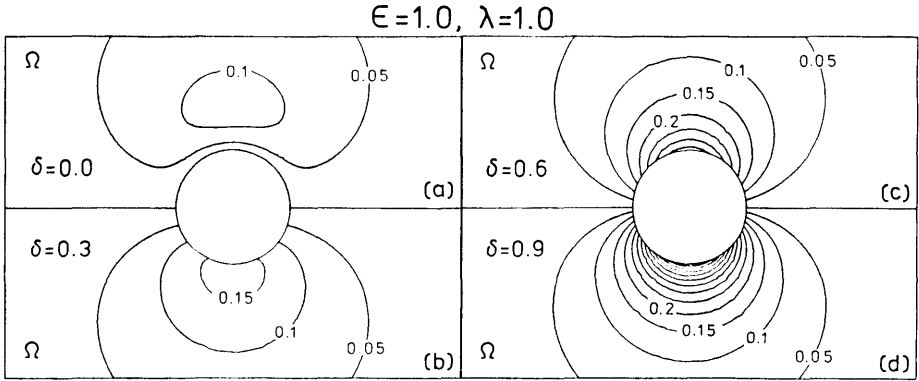


Fig. 10. Equi-microrotation lines

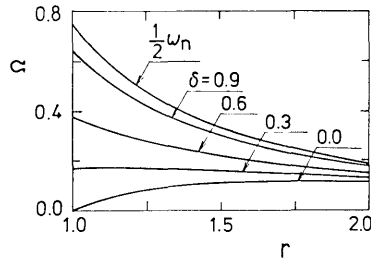


Fig. 11. Distributions of microrotation ( $\theta=90^\circ, \lambda=1.0, \epsilon=1.0$ )

$$\Omega(\delta=1) = \frac{3 \sin \theta}{4} \cdot \frac{1}{r^3}. \quad (52)$$

In this case,  $\Omega$  equals  $\omega_n/2$ , while taking  $\delta \rightarrow 0$  yields the increase of the difference between  $\Omega$  and  $\omega/2$ . Now let us consider the relation between  $\delta$  and the concentration of corpuscles. As the concentration approaches to zero, one expects the microrotation to approach the local fluid vorticity. On the other hand as the concentration approaches maximum, one expects the microrotation to decrease because of interactions of corpuscles. Thus it seems that  $\delta \rightarrow 0$  and  $\delta \rightarrow 1$  correspond to the concentrated and the diluted solutions, respectively. In view of the above discussions it is natural that some physical relations between  $\delta$  and the concentration of corpuscles are postulated. This relation is indicated by Allen and Kline (1968), and Kline, Allen and DeSilva (1968). However more experimental investigations will be necessary in order to clarify these relations.

### 5.3 Drag on a sphere

The force exerted by the fluid on a sphere is

$$\mathbf{f} = \int_s \mathbf{n} \cdot \mathbf{T} ds, \quad (53)$$

where  $\mathbf{n}$  is the unit outer normal to the surface of the sphere and the integration is to taken around the whole surface of the sphere. Substituting the constitutive equation into Eq. (53) leads to (see Tanahashi (1979)<sup>(22)</sup>)

$$\mathbf{f} = -\int_s p \mathbf{n} ds + (\mu + \mu_1) \int_s \boldsymbol{\omega} \times \mathbf{n} ds - 2\mu_1 \int_s \boldsymbol{\Omega} \times \mathbf{n} ds. \quad (54)$$

The drag acting on the sphere is given by

$$D = \mathbf{f} \cdot (-\mathbf{e}_z). \quad (55)$$

From Eqs. (54) and (55), the drag is given by

$$D_p = \frac{1}{3} \cdot \frac{(\lambda+1)\{\varepsilon(1-\delta)+1\}}{\lambda\{\varepsilon(1-\delta)+1\}+1}, \quad (56)$$

$$D_f = 2D_p, \quad (57)$$

so that the total drag is

$$D = D_p + D_f = 3D_p. \quad (58)$$

Thus the ratio of pressure drag to frictional drag is 2:1 which is the same for Newtonian fluid. Influences of three parameters on the drag are shown in Figs. 12 and 13. From Fig. 12, the drag is nearly proportional to  $\varepsilon$ . When  $\lambda > 7$ , the drag is approximately constant.

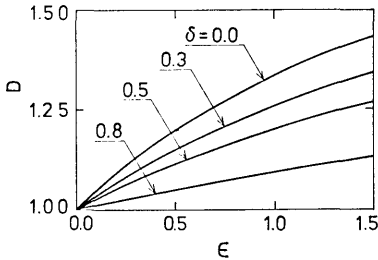


Fig. 12. Drag ( $\lambda=1.0$ )

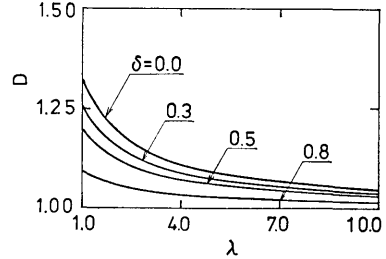


Fig. 13. Drag ( $\varepsilon=1.0$ )

Apparent viscosity in this case can be defined as follows :

$$D = 6\pi\mu_a U a, \quad (59)$$

where the drag  $D$  is the dimensional form. Hence Eqs. (58) and (59) show that the ratio of the apparent viscosity to the viscosity is equal to the total drag :

$$\frac{\mu_a}{\mu} = D. \quad (60)$$

## 6. Summary and Concluding Remarks

In the present paper, the Stokesian flow past a stationary sphere is investigated.

The intermediate spin boundary condition between zero spin and zero antisymmetric stress tensor is used here by introducing a wall-condition parameter, which was applied to shearing flow problems by Allen and Kline (1968). By introducing a vector potential instead of a stream function, velocity, vorticity, microrotation and drag on the sphere are mathematically obtained. When  $\varepsilon \rightarrow 0$ ,  $\lambda \rightarrow \infty$  or  $\delta \rightarrow 1$ , velocity profiles approach those of Newtonian fluid. There is little significant difference of stream lines between micropolar fluid and Newtonian fluid. It appears that  $\varepsilon$  hardly affects on  $\Omega$ , that the area over which  $\Omega \approx \omega_n/2$  is valid expands toward the sphere as increase of  $\lambda$ , and that distributions of  $\Omega$  alter sensitively with  $\delta$  in the whole field. The characteristics of  $\varepsilon$ ,  $\lambda$  and  $\delta$  are summarized as follows:

- (1) The ratio  $\varepsilon$  of viscosities represents the influence of antisymmetric part of stress tensor and it means the frictional effect between corpuscle and fluid.
- (2) The size effect parameter  $\lambda$  reveals the relative relation of the sizes between corpuscle and sphere.
- (3) Some relations between the wall-condition parameter  $\delta$  and the concentration of corpuscles can be postulated. But many experimental investigations are necessary in order to make these relations clear in detail.

Finally, the ratio of pressure drag to frictional drag on a sphere is 2:1 which is identical to that for Newtonian fluid.

### Acknowledgments

The authors express their appreciation to Mr. A. Kobayashi and Mr. Y. Tomoda who drew painstakingly most of figures. The authors also wish to acknowledge that a part of numerical calculation, editing and typing of this manuscript were made with the aid of the word-processor of HITAC M-280 H of Tokyo University Large-Capacity Computer Center.

### REFERENCES

- [1] Aero, E.L., et al., *J. Appl. Math. Mech.*, Vol. 29, No. 2 (1965), pp. 333-346.
- [2] Allen, S.J. and Kline, K.A., *Trans. Soc. Rheol.*, Vol. 12, No. 3 (1968), pp. 457-468.
- [3] Allen, S.J., et al., *Trans. Soc. Rheol.*, Vol. 15, No. 1 (1971), pp. 177-188.
- [4] Ariman, T., *J. Biomech.*, Vol. 4, No. 3 (1971), pp. 185-195.
- [5] Ariman, T., et al., *Trans. ASME, J. Appl. Mech.*, Vol. 41, No. 1 (1974), pp. 1-7.
- [6] Brenner, H., *J. Colloid and Interface Sci.*, Vol. 32, No. 1 (1970), pp. 141-158.
- [7] Brenner, H. and Weissman, M.H., *J. Colloid and Interface, Sci.*, Vol. 41, No. 3 (1972), pp. 499-531.
- [8] Bugliarello, G. and Sevilla, J., *Biorheology*, Vol. 7, No. 2 (1970), pp. 85-107.
- [9] Condiff, D.W. and Dahler, J.S., *Phys. Fluids*, Vol. 7, No. 6 (1964), pp. 842-854.
- [10] Cowin, S.C., *Biorheology*, Vol. 9 (1972), pp. 23-25.
- [11] Eringen, A.C., *J. Math. & Mech.*, Vol. 16, No. 1 (1966), pp. 1-18.
- [12] Kamiyama, S., et al., *Bull. JSME*, Vol. 22, No. 171 (1979), pp. 1205-1211.
- [13] Kirwan, A.D., Jr. and Newman, N., *Int. J. Eng. Sci.*, Vol. 7, No. 8 (1969), pp. 883-893.
- [14] Kline, K.A. and Allen, S.J., *Biorheology*, Vol. 6, No. 2 (1969), pp. 99-108.
- [15] Kline, K.A., et al., *Biorheology*, Vol. 5, No. 2 (1968), pp. 111-118.

## Stokesian Flow of a Micropolar Fluid

- [16] Kline, K.A., et al., *Biorheology*, Vol. 9, No. 1 (1972), pp. 1-22.
- [17] McTague, J.P., *J. Chem. Phys.* Vol. 51, No. 1 (1969), pp. 133-136.
- [18] Neuringer, J.L. and Rosensweig, R. E., *Phys. Fluids*, Vol. 7, No. 12 (1964), pp. 1927-1937.
- [19] Ramkissoon, H. and Majumdar, S.R., *Letters Appl. Eng. Sci.*, Vol. 13 (1975), pp. 133-142.
- [20] Shliomis, M.I., *Sov. Phys. JETP*, Vol. 34, No. 6 (1972), pp. 1291-1294.
- [21] Stokes, V.K., *Phys. Fluids*, Vol. 14, No. 7 (1971), pp. 1580-1582.
- [22] Tanahashi, T., *Sci. Machine*, Vol. 31, No. 9 (1979), pp. 1059-1063.
- [23] Tanahashi, T., et al., *Trans. Jpn. Soc. Mech. Eng., Ser. B*, Vol. 49, No. 437 (1983), pp. 53-61.
- [24] Tomita, Y., et al., *Prepr. of Jpn. Soc. Mech. Eng.*, No. 810-8 (1981), pp. 1-3.